# Test of macroscopic realism with coherent light

Hui Wang,<sup>1,2</sup> Shuang Wang,<sup>1</sup> and Cong-Feng Qiao<sup>1,\*</sup>

<sup>1</sup>School of Physical Sciences & Key Laboratory of Vacuum Physics, University of Chinese Academy of Sciences, YuQuan Road 19A, Beijing 100049, China

> <sup>2</sup>International Centre for Theoretical Physics Asia-Pacific, University of Chinese Academy of Sciences, Beijing 100190, China

Macro-realism is a fundamental feature of classical world that contradicts with the quantum theory. An elegant method of testing macrorealism is to apply the Leggett-Garg inequality (LGI), but the non-invasivity of measurement is challenging in practice. In this work, we report the LGI violation of path observable in a composite interference experiment with coherent light. Experiment results confirm the occurrence of destructive interference providing per se as evidence of macro-realism violation. And by using an exact weak measurement model in the present experiment, the advantage that the violation of realism is independent of the invasive strength allows the realization of direct measurement and strengthens the persuasion of verification at the macroscopic scale.

### I. INTRODUCTION

In 1985, Leggett and Garg provided an elegant method to experimentally test macrorealism with a class of inequalities [1]. The Leggett-Garg inequalities (LGIs) are based on the following two assumptions. (1) Macrorealism per se (MRps): A macroscopic system always remains in one of its available two or more distinct ontic states. (2) Noninvasive measurability (NIM): In principle, it is possible to determine the state of macrosystem without disturbing it. The classical world we daily experience intuitively obeys these assumptions, while quantum mechanics is not satisfied because of the superposition principle and the collapse of state. Hence the LGIs act as an indicator of the existence of coherence, and test the applicability of quantum mechanics when scaling from microscopic to macroscopic systems [2].

Considering dichotomic observable  $\hat{M} = \pm 1$  in macrorealistic system, the standard LGI for the *n*-time measurement is given by [3]

$$K_n = \left\langle \hat{M}_1 \hat{M}_2 \right\rangle + \left\langle \hat{M}_2 \hat{M}_3 \right\rangle + \dots + \left\langle \hat{M}_{n-1} \hat{M}_n \right\rangle - \left\langle \hat{M}_1 \hat{M}_n \right\rangle. \tag{1}$$

Here,  $\langle \hat{M}_i \hat{M}_j \rangle = \sum_{m_i,m_j} m_i m_j P\left(M_i^{m_i},M_j^{m_j}\right)$  is the correlation function, where  $P\left(M_i^{m_i},M_j^{m_j}\right)$  is the joint probability of obtaining measurement  $m_i$  and  $m_j$  at sequential time  $t_i$  and  $t_j$ . The bound of inequality (1) is formulated as follows [4]. If n is odd,  $-n \leqslant K_n \leqslant n-2$ , and if n is even,  $-(n-2) \leqslant K_n \leqslant n-2$ . For n=3, the typical LGI is written as

$$K_3 = \left\langle \hat{M}_1 \hat{M}_2 \right\rangle + \left\langle \hat{M}_2 \hat{M}_3 \right\rangle - \left\langle \hat{M}_1 \hat{M}_3 \right\rangle, \qquad (2)$$

and satisfies  $-3 \leqslant K_3 \leqslant 1$ . However, the LGI will go beyond bound if the system is quantum. For a two-level system, the maximum quantum value of n-time case

is  $(K_n)_Q = n\cos\frac{\pi}{n}$ , which is referred to as the Lüders bound [5]. For  $K_3$  and  $K_4$  the Lüders bound are 1.5 and  $2\sqrt{2}$ , respectively. Recently, it has been predicted that the quantum violation value can exceed Lüders bound. One is to relax the measurement assumption from the Lüders state-update rule to a general projective measurement for multilevel system, e.g.,  $K_3^{\max} = 1.7565$  in three-level system [6]. The other is the new variant of LGI with three-time, two-time, and one-time correlation function, where  $K_3^{\max} = 1.93$  [7].

In terms of experiment, the primary and decisive condition for verifying macroscopic realism is the implementation of NIM assumption, which is also the main challenge in practice. Specific methods include ideal negative result measurement (INRM) [8] and weak measurement [9, 10]. The former confirm that there is no interaction between the measured system and the auxiliary instrument by keeping only the negative results. The latter, in principle, is capable of imposing an extrem-weak disturbance on system state. Up to now, LGI has been experimentally tested in a variety of microsystems, i.e. nuclear spins [11–13], nitrogen-vacancy center [14], single photons [15–17], superconducting flux qubit [18], and light-matter interaction [19]. The results indicate the violations of LGI for each individual quantum measurement, but it does not sufficiently infer that it also holds in macroscopic system, e.g., an ensemble of photons.

With the exception of quantum system, the LGI gains new focus on classical optical system [20, 21]. Experiments investigated the violation of LGI by using the polarization freedom degree of the laser beam [22]. However, the lack of quantification of invasiveness introduced by the measurement instrument is an obvious loophole and fails to satisfy the assumption of NIM. In our work, this loophole is closed by exploiting weak measurement technique.

Recently, A. K. Pan. proposed a new correlation between interference experiment and the violation of LGI with the assistance of anomalous weak value, which sug-

<sup>\*</sup>Electronic address: qiaocf@ucas.ac.cn

gested the avoidance of the NIM assumption [23]. However, achieving it in experiment is hardly available. Here we tested this LGI variant in the path interference experiment of classical light. Results show the existence of anomalous weak value is alway accompanied by destructive interference, and consequently, LGI is identified to be violated in this range. Differ from the previous ones, violation of macro-realism is inferred straight from the destructive interference per se. Therefore, we implement a direct test for the macroscopic realism by using precise weak measurement.

#### II. THEORY AND METHODOLOGY

In this section, we prior to review the derivation in Ref. [23]. The LGI for the three-time measurement scenario can also be expressed as

$$K_{3} = 1 - m_{1}m_{2} \left\langle \hat{M}_{1}\hat{M}_{2} \right\rangle - m_{2}m_{3} \left\langle \hat{M}_{2}\hat{M}_{3} \right\rangle + m_{1}m_{3} \left\langle \hat{M}_{1}\hat{M}_{3} \right\rangle \geqslant 0,$$

$$(3)$$

where  $m_i m_j = \pm 1 (i, j = 1, 2, 3)$ . Specially,  $m_1 = m_2 = m_3 = 1$ , one simply recovers inequality (2).

The measurement  $\hat{M}_1$  at  $t_1$  directly satisfy  $\hat{M}_1 |+m_1\rangle = |+m_1\rangle$  and  $m_1 = +1$  when the initial system is prepared at particular state  $|\psi_i\rangle = |+m_1\rangle$ . Hence for different values of  $m_2 = \pm 1$  and  $m_3 = \pm 1$ , Eq. (3) evolved into four two-time LGIs

$$K_{31} = 1 - \left\langle \hat{M}_{2} \right\rangle - \left\langle \hat{M}_{2} \hat{M}_{3} \right\rangle + \left\langle \hat{M}_{3} \right\rangle \geqslant 0,$$

$$K_{32} = 1 + \left\langle \hat{M}_{2} \right\rangle + \left\langle \hat{M}_{2} \hat{M}_{3} \right\rangle + \left\langle \hat{M}_{3} \right\rangle \geqslant 0,$$

$$K_{32} = 1 - \left\langle \hat{M}_{2} \right\rangle + \left\langle \hat{M}_{2} \hat{M}_{3} \right\rangle - \left\langle \hat{M}_{3} \right\rangle \geqslant 0,$$

$$K_{34} = 1 + \left\langle \hat{M}_{2} \right\rangle - \left\langle \hat{M}_{2} \hat{M}_{3} \right\rangle - \left\langle \hat{M}_{3} \right\rangle \geqslant 0.$$

$$(4)$$

In fact, there is only one output per measurement, so inequalities (4) are impossible to hold at the same time. Mathematically articulated as  $\hat{M}_3 = 2 |+m_3\rangle \langle +m_3| - \mathbb{I} = \mathbb{I} - 2| - m_3\rangle \langle -m_3|$ . So, the projective measurement of  $\hat{M}_3$  at time  $t_3$  is performed by  $|\psi_f\rangle = |+m_3\rangle$  or  $|-m_3\rangle$ . The process of setting a fixed option at initial and last time, in essence, provide preand post-selective state for weak measurement. Under the constraint of a two-state vector, the left sides of above

four LGIs are manipulate as

$$(K_{31})_{Q} = 2p_{|+m_{3}\rangle} \left[ 1 - \left\langle \hat{M}_{2} \right\rangle_{w}^{|+m_{3}\rangle} \right],$$

$$(K_{32})_{Q} = 2p_{|+m_{3}\rangle} \left[ 1 + \left\langle \hat{M}_{2} \right\rangle_{w}^{|+m_{3}\rangle} \right],$$

$$(K_{33})_{Q} = 2p_{|-m_{3}\rangle} \left[ 1 - \left\langle \hat{M}_{2} \right\rangle_{w}^{|-m_{3}\rangle} \right],$$

$$(K_{34})_{Q} = 2p_{|-m_{3}\rangle} \left[ 1 + \left\langle \hat{M}_{2} \right\rangle_{w}^{|-m_{3}\rangle} \right],$$

$$(5)$$

where  $\langle \hat{M}_2 \rangle_w^{|\pm m_3 \rangle} = \frac{\langle \pm m_3 | \hat{M}_2 | + m_1 \rangle}{\langle \pm m_3 | + m_1 \rangle}$  is the weak value of  $\hat{M}_2$  and  $p_{|\pm m_3 \rangle} = |\langle \pm m_3 | + m_1 \rangle|^2$  is the postselection probability. The formula (5) contains the association between LGI, weak value and postselection probability. It can be inferred that the LGI will be violated that  $(K_{3i})_Q < 0$  when the weak value exceed eigenvalue range [-1, 1].

There is an emphasis on path-only interference experiment in Ref. [23]. That is, the NIM assumption is dispensable because no additional measurement apparatus is introduced. In the Mach-Zehender (MZ) set up, the initial system state is  $|\psi_i\rangle = \cos\theta \,|U\rangle + \sin\theta \,|D\rangle$ , where  $\{|U\rangle,|D\rangle\}$  are orthogonal path states. And the projected states are  $|+m_3\rangle = (|U\rangle + |D\rangle)/\sqrt{2}, \, |-m_3\rangle = (|U\rangle - |D\rangle)/\sqrt{2}$  with the probabilities of  $p_{|+m_3\rangle} = (1+\sin 2\theta)/2$  and  $p_{|-m_3\rangle} = (1-\sin 2\theta)/2$ , respectively. Thus, for the dichotomic observable  $\hat{M}_2 = |U\rangle\langle U| - |D\rangle\langle D|$ , a simple substitution Eq. (5) turns to

$$(K_{31})_Q = 2\sin\theta(\cos\theta + \sin\theta),$$

$$(K_{32})_Q = 2\cos\theta(\cos\theta + \sin\theta),$$

$$(K_{33})_Q = 2\sin\theta(\sin\theta - \cos\theta),$$

$$(K_{34})_Q = 2\cos\theta(\cos\theta - \sin\theta).$$
(6)

Here, weak value  $\langle \hat{M}_2 \rangle_w^{|+m_3\rangle} = (\cos \theta - \sin \theta)/(\cos \theta + \sin \theta)$  and  $\langle \hat{M}_2 \rangle_w^{|-m_3\rangle} = (\cos \theta + \sin \theta)/(\cos \theta - \sin \theta)$  are real.

The path-only scheme is logical in theory, but for this procedure to work, one has to consider the setting of weak disturbance and variable  $\theta$ . In this context, we adopt the exact weak measurement method and regulate parameter  $\theta$  with the polarization degrees of freedom [24]. A particularly notable feature of this experimental design is that the weak value of Pauli type observable is independent of the coupling strength. It is further deduced that the results are consistent whether the perturbation is present or absent. This effect is similar to the case of path-only interference, i.e., avoiding the use of NIM. In other words, the test for macroscopic realism can be done directly.

Following the above motivation, the experimental setup is implemented by a controlled interference network as depicted in Fig. 1. The optical interference

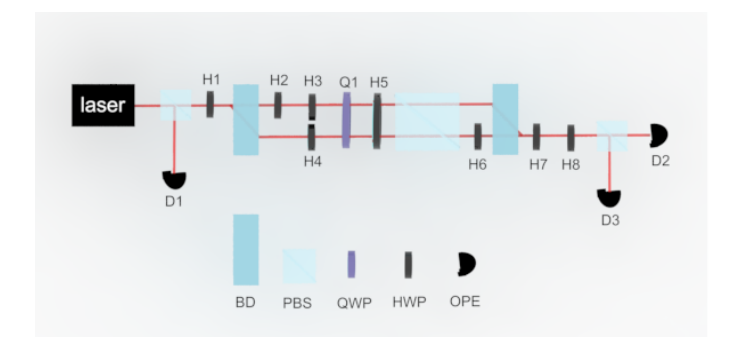


Figure 1: Experimental setup. The laser is prepared to the state  $|\psi\rangle=\cos\theta\,|H\rangle+\sin\theta\,|V\rangle$  through a polarizing beam splitter (PBS) and half wave plate (H1). Then it enters an interference network consists of two polarizing beam displacers (BD), where polarization and path degrees of freedom act as pointer and measured system. Sets of H3 and H4 on the upper and lower path are used to realize the weak interaction  $\hat{\bf U}$ . Projective measurement of pointer is performed via Q1, H5, and PBS. Finally, the multiple waveplates (H6-8), BD and PBS are applied to generate the post-selection state  $|\psi_f\rangle=|\pm m_3\rangle$ .

consists of two polarizing beam displacers (BDs) and multiple waveplates. BDs can transmit vertical polarized light directly and deflect horizontal light laterally by the displacement of 4 mm. The laser beam passes through polarizing beam splitter (PBS) and followed half wave plate (HWP, H1) with the setting angle  $\theta/2$  in the transmission path, providing the linearly polarized state  $|\psi\rangle = \cos\theta |H\rangle + \sin\theta |V\rangle$ . The reflection path of PBS serves as a reference and records the fluctuation of light intensity. The first BD splits the state  $|\psi\rangle$  into two parallel spatial modes, upper mode and lower mode encoded as  $|U\rangle$  and  $|D\rangle$ , respectively. Then the polarization information  $\{|H\rangle, |V\rangle\}$  transform into  $\{|U\rangle, |D\rangle\}$  via the H2 rotated at  $\pi/4$  in the upper path. The pre-selected state  $|\psi_i\rangle$  and pointer state  $|H\rangle$  are prepared. So the composite state combined with the pointer and measured system is clearly expressed as  $|H\rangle(\cos\theta|U\rangle + \sin\theta|D\rangle)$ at the initial time. Subsequently, the weak interaction  $\hat{\mathbf{U}} = e^{-i\gamma \hat{M}_2 \otimes \hat{\sigma}_y}$  is realized by placing H3(  $\gamma/2$ ) and H4(  $-\gamma/2$ ) on the upper and lower path, respectively.

Following the preparation method of pre-selected state, the post-selection state is done through BD2, HWPs (H6-8) and PBS, where H6(H7) and H8 are rotated at  $\pi/4$  and  $\pi/8$  radians, respectively. The detection ports D2 and D3 correspond to the projection basis of system  $|+m_3\rangle$  and  $|-m_3\rangle$ . As a result, the information of the measured system (weak value) is captured in the pointer state. More explicitly, the relation between weak value  $\langle \hat{M}_2 \rangle_w$  and the expectation value of pointer observable  $\langle \hat{\sigma}_i \rangle_p$  is exactly

expressed as [24]

$$\langle \hat{\sigma}_x \rangle_p = \frac{\sin 2\gamma \operatorname{Re} \langle \hat{M}_2 \rangle_w}{\cos^2 \gamma + \sin^2 \gamma |\langle \hat{M}_2 \rangle_w|^2},$$

$$\langle \hat{\sigma}_y \rangle_p = \frac{\sin(2\gamma) \operatorname{Im} \langle \hat{M}_2 \rangle_w}{\cos^2 \gamma + \sin^2 \gamma |\langle \hat{M}_2 \rangle_w|^2}.$$
(7)

According to the formula (7), the real and imaginary part of weak value can be extracted from

$$\langle \hat{\sigma}_x \rangle_p = \frac{(I_+ - I_-)}{(I_+ + I_-)} \qquad \langle \hat{\sigma}_y \rangle_p = \frac{(I_R - I_L)}{(I_R + I_L)}, \qquad (8)$$

where the intensity at the corresponding polarization is denoted by  $I_i$ , the polarization  $|\pm\rangle = \frac{1}{\sqrt{2}}(|H\rangle \pm |V\rangle)$  and  $|L(R)\rangle = \frac{1}{\sqrt{2}}(|H\rangle \pm i|V\rangle)$ . So, the quarter-wave plate (Q1), H5, and PBS are set to realize the projection measurement of pointer  $\{|+\rangle, |-\rangle\}$  and  $\{|R\rangle, |L\rangle\}$ . Note that the projection measurement was preferentially performed in the experiment setup, because it is physically commutable with the post-selection of measured system. It does not affect the measurement result for which one is performed in priority.

#### III. RESULTS

According to Eq.(7, 8), the weak value  $\langle \hat{M}_2 \rangle_w$  and the LGIs (5) for quantum systems are calculated based on the light intensity detected by the optical power meter (OPE). And the measurement strength, which is continuously adjustable by parameter  $\gamma$ , is typically taken at 12° in Fig. 2 and Fig. 3.

Figure 2 show the experimental results of the real and imaginary part of weak value as well as the post-selection probability. The experimental imaginary part  $\text{Im}\langle \hat{M}_2 \rangle_w^{|\pm m_3\rangle}$  is nearby-zero, which is consistent with the theoretical prediction that the weak value is real. When the post-selection probability satisfy  $p_i < 0.5$ , the real part is either  $\text{Re}\langle \hat{M}_2 \rangle_w^{|\pm m_3\rangle} > 1$  or  $\text{Re}\langle \hat{M}_2 \rangle_w^{|\pm m_3\rangle} < -1$ . That is to say, it will be accompanied by an anomalous weak value if there is destructive interference at the detection port. We noticed that the postselection probability can be amplified by N times while the weak value remains fixed [25, 26]. For example, the dashed cyan and magenta lines in Fig. 2.(a) correspond to magnification N=2 and N=3, denoted by  $p_{|+m_3\rangle}^{N=2}$  and  $p_{|+m_3\rangle}^{N=3}$ , respectively. It also can be seen that an anomalous weak value exist once the post-selection probability is less than half of the maximum value.

The corresponding results of LGIs (6) are shown in Fig. 3, where the dashed curves are the theoretical prediction and the symbols are the experimental values. Fig. 3(**a**) and 3(**b**) display the values of  $(K_{3i})_Q(i=1,2)$ 

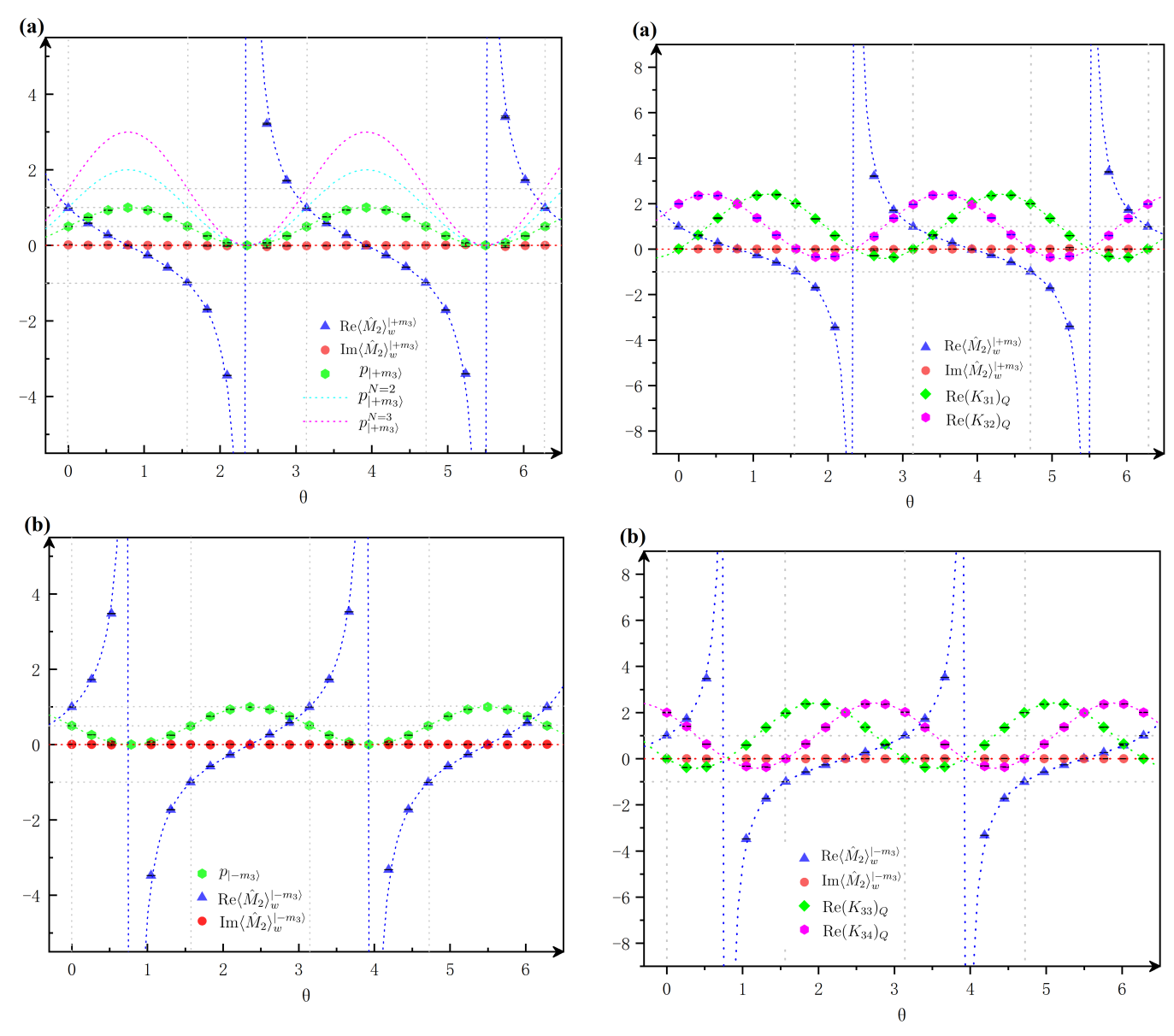


Figure 2: Experimental results of the post-selection probability p and weak value  $\langle \hat{M}_2 \rangle_w$ . The dashed curves represent theoretical prediction, while the symbols are the experimental values. (a) At the post-selective state  $|+m_3\rangle$ . (b) At the post-selective state  $|-m_3\rangle$ . Obviously, the anomalous weak values exist when the post-selection probability is less than half of the maximum value. Error bars indicate  $\pm 1$  standard deviation.

and 3, 4),  $\operatorname{Re}\langle \hat{M}_2 \rangle_w$  and  $\operatorname{Im}\langle \hat{M}_2 \rangle_w$  for post-selective state  $|+m_3\rangle$  and  $|-m_3\rangle$ , respectively. There is definitely an anomalous weak value when one of the equations satisfies  $(K_{3i})_Q < 0$ , since LGIs (4) cannot hold simultaneously. Conversely, the existence of anomalous weak value certainly indicates the violation of a specific LGI. Conjoined with the results of Fig. 2, it suggests that whenever the destructive effect is observed in the interference, anomalous weak values exist and the violation of LGI is further obtained. These values thus show clear experimental ev-

Figure 3: The results of the verification of LGIs (6). (a) The experimental values of  $(K_{31})_Q$  and  $(K_{32})_Q$  with post-selective state  $|+m_3\rangle$ . (b) The experimental values of  $(K_{33})_Q$  and  $(K_{34})_Q$  with post-selective state  $|-m_3\rangle$ . The symbols and dashed curves represent the experimental values and theoretical predictions. There is a violation of LGI in the range of anomalous weak values. Conversely, violation determine that the weak value is anomalous. Error bars indicate  $\pm 1$  standard deviation.

idence that the macrorealism is verified by using interference experiment with weak measurement.

On the other hand, to verify the dispensability of NIM, different coupling strengths suffered by the measured system need to be allowed. Therefore, we set the pre- and post-selection states as  $|\psi_i\rangle = (0.966 |U\rangle + 0.259 |D\rangle)$ ,  $|\psi_f\rangle = |+m_3\rangle$ . Fig. 4 shows the experimental obtained

values of  $|\langle \hat{M}_2 \rangle_w^{|+m_3} \rangle|^2$ ,  $\text{Re} \langle \hat{M}_2 \rangle_w^{|+m_3} \rangle$  and  $\text{Im} \langle \hat{M}_2 \rangle_w^{|+m_3} \rangle$  for different measurement strength  $\gamma$  in the range of 24° to  $-24^\circ$  with the step of 4°. The weak value keep constant with the varying strength, which is in accordance with its definition. In fact, the experiment allows setting arbitrary coupling strengths even infinitely close to zero, while do not altering the results. Because the Eq. (7) for two-dimensional observable  $\hat{M}_2$  is obtained without approximation. That is a favorable condition, compared with the previous weak measurement method that required the perturbation to be within the linear-response regime [27, 28]. Such an advantage moves further toward the initial purpose of the NIM assumption, resulting in a direct test of macroscopic realism.

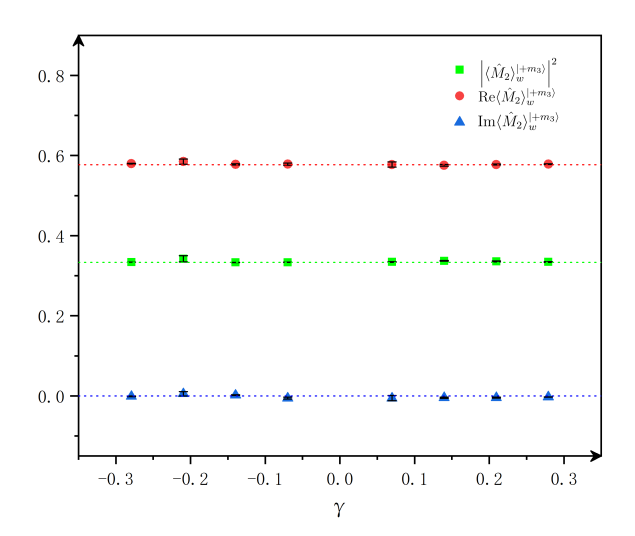


Figure 4: Experimental results of weak value  $\langle \hat{M}_2 \rangle_w^{|+m_3\rangle}$  at varying coupling strength  $\gamma$ . The dashed green, blue and red curves represent the norm, imaginary and real part of theoretical values, labeled as  $|\langle \hat{M}_2 \rangle_w^{|+m_3\rangle}|^2$ ,  $\text{Re} \langle \hat{M}_2 \rangle_w^{|+m_3\rangle}$  and  $\text{Im} \langle \hat{M}_2 \rangle_w^{|+m_3\rangle}$ . The symbols represent experimental values. It is evident that the weak value are independent of coupling strength. Error bars indicate  $\pm 1$  standard deviation.

The error bars in figures are calculated by the error propagation formula. Considering the imperfectness of calibration or the slowly drift and slight vibrating of the interferometer in the measurement duration, the corresponding experimental data agrees with the theoretical prediction.

## IV. CONCLUSION

In this work, we have experimentally demonstrated the violation of the Leggett-Garg inequality for path observable in a composite interference network, which consist of polarization and path degrees of freedom. Results confirm that the existence of destructive interference inherently implies a violation of macro-realism. Furthermore, the present experiment complements the loopholes of previous ones [22] with precise weak measurement, i.e., the realism has convincingly demonstrated in the macroscopic scale using classical coherent light. Another salient feature is that results of LGI violation always hold and remain constant even if a perturbation of arbitrary strength is introduced into the system. Our tests therefore achieve a direct measurement whereby the violation of a macrorealist inequality is only caused by the violation of realism per se, releasing the requirement of the NIM assumption. This may not only provoke deep thought on the relation between macroscopic coherence and quantum fundamental issue, but also enrich the applications in quantum information processing.

## Acknowledgements

This work was supported in part by the National Natural Science Foundation of China(NSFC) under the Grants 11975236, 12235008 and by the University of Chinese Academy of Sciences.

A. J. Leggett and A. Garg, Quantum Mechanics Versus Macroscopic Realism: Is the Flux There When Nobody Looks? Phys. Rev. Lett. 54, 857 (1985).

<sup>[2]</sup> A. J. Leggett, Testing the limits of quantum mechanics: motivation, state of play, prospects, J. Phys.: Condens. Matter 14, R415 (2002).

<sup>[3]</sup> V. Athalye, S. S. Roy and T. S. Mahesh, Investigation of the Leggett-Garg Inequality for Precessing Nuclear Spins, Phys. Rev. Lett. 107, 130402 (2011).

<sup>[4]</sup> C. Emary, N. Lambert and F. Nori, Leggett-Garg inequalities, Rep. Prog. Phys. 77, 016001 (2014).

<sup>[5]</sup> C. Budroni, T. Moroder, M. Kleinmann, and O. Gühne, Bounding Temporal Quantum Correlations, Phys. Rev.

Lett. 111, 020403 (2013).

<sup>[6]</sup> C. Budroni and C. Emary, Temporal Quantum Correlations and Leggett-Garg Inequalities in Multilevel Systems, Phys. Rev. Lett. 113, 050401 (2014).

<sup>[7]</sup> A. K. Pan, M. Qutubuddin, and S. Kumari, Quantum violation of variants of Leggett-Garg inequalities up to the algebraic maximum for a qubit system, Phys. Rev. A 98, 062115 (2018).

<sup>[8]</sup> G. C. Knee, S. Simmons, E. M. Gauger, J. J. L. Morton, H.Riemann, N. V. Abrosimov, P. Becker, H.-J. Pohl, K. M. Itoh, M. L. W. Thewalt, G. A. D. Briggs, and S. C. Benjamin, Violation of a Leggett-Garg inequality with ideal non-invasive measurements, Nat. Commun. 3, 606

- (2012).
- [9] M. E. Goggin, M. P. Almeida, M. Barbieri, B. P. Lanyon, J. L. O'Brien, A. G. White, and G. J. Pryde, Violation of the Leggett-Garg inequality with weak measurements of photons. Proc. Natl Acad. Sci. 108, 1256 (2011).
- [10] J. Dressel, C. J. Broadbent, J. C. Howell, and A. N. Jordan, Experimental Violation of Two-Party Leggett-Garg Inequalities with Semiweak Measurements, Phys. Rev. Lett. 106, 040402 (2011).
- [11] V. Athalye, S. S. Roy, and T. S. Mahesh, Investigation of the Leggett-Garg Inequality for Precessing Nuclear Spins, Phys. Rev. Lett. 107, 130402 (2011).
- [12] H. Katiyar, A. Shukla, K. R. K. Rao, and T. S. Mahesh, Violation of entropic Leggett-Garg inequality in nuclear spins, Phys. Rev. A 87, 052102 (2013).
- [13] H. Katiyar, A. Brodutch, D. Lu, and R. Laflamme, Experimental violation of the Leggett-Garg inequality in a three-level system, New J. Phys. 19, 023033 (2017).
- [14] M. Tusun, W. Cheng, Z. Chai, Y. Wu, Y. Wang, X. Rong, J. F. Du, Experimental violation of the Leggett-Garg inequality with a single-spin system, Phys. Rev. A 105, 042613 (2022).
- [15] K. Wang, C. Emary, M. Xu, X. Zhan, Z. Bian, L. Xiao, and P. Xue, Violations of a Leggett-Garg inequality without signaling for a photonic qutrit probed with ambiguous measurements, Phys. Rev. A 97, 020101 (2018).
- [16] K. Wang, M. Xu, L. Xiao, and P. Xue, Experimental violations of Leggett-Garg inequalities up to the algebraic maximum for a photonic qubit, Phys. Rev. A 102, 022214 (2020).
- [17] K. Joarder, D. Saha, D. Home, and U. Sinha, Loophole-Free Interferometric Test of Macrorealism Using Heralded Single Photons, PRX Quantum 3, 010307 (2022).
- [18] G. C. Knee, K. Kakuyanagi, M.-C. Yeh, Y. Matsuzaki, H. Toida, H. Yamaguchi, S. Saito, A. J. Leggett, and W. J. Munro, A strict experimental test of macroscopic realism in a superconducting flux qubit. Nat Commun. 7, 13253 (2016).

- [19] Z. Q. Zhou, S. F. Huelga, C. F. Li, and G. C. Guo, Experimental Detection of Quantum Coherent Evolution Through the Violation of Leggett-Garg-Type Inequalities, Phys. Rev. Lett. 115, 113002 (2015).
- [20] X. Zhang, T. Li, Z. Yang, and X. Zhang, Experimental observation of the Leggett-Garg inequality violation in classical light, J. Opt. 21, 015605 (2019).
- [21] H. Chevalier, A. J. Paige, H. Kwon, and M. S. Kim, Violating the Leggett-Garg inequalities with classical light, Phys. Rev. A 103, 043707 (2021).
- [22] W. L. Zhang, R. K. Saripalli, J. M. Leamer, R. T. Glasser, and D. I. Bondar, Experimental violation of the Leggett-Garg inequality using the polarization of classical light, Phys. Rev. A 104, 043711 (2021).
- [23] A. K. Pan, Interference experiment, anomalous weak value, and Leggett-Garg test of macrorealism, Phys. Rev. A 102, 032206 (2020).
- [24] J. S. Chen, M. J. Hu, X. M. Hu, B. H. Liu, Y. F. Huang, C. F. Li, G. C. Guo, and Y. S. Zhang, Experimental realization of sequential weak measurements of non-commuting Pauli observables, Opt. Express 27, 6089 (2019).
- [25] J. S. Chen, B. H. Liu, M. J. Hu, X. M. Hu, C. F. Li, G. C. Guo, and Y. S. Zhang, Realization of entanglement-assisted weak-value amplification in a photonic system, Phys. Rev. A 99, 032120 (2019).
- [26] Y. Kim, S. Y. Yoo, and Y. H. Kim, Heisenberg-Limited Metrology via Weak-Value Amplification without Using Entangled Resources, Phys. Rev. Lett. 128, 040503 (2022).
- [27] A. G. Kofman, S. Ashhab, and F. Nori, Nonperturbative theory of weak pre-and post-selected measurements, Phys. Rep. 520, 43 (2012).
- [28] J. Dressel, M. Malik, F. M. Miatto, A. N. Jordan, and R. W. Boyd, Colloquium: Understanding quantum weak values: Basics and applications, Rev. Mod. Phys. 86, 307 (2014).